ЯДЕРНА ФІЗИКА

УДК 539.173

R. N. Panda[1], M. Bhuyan[2], S. K. Patra[3]

[1] Department of Physics, Institute of Technical Education and Research, Siksha O Anusandhan University, Bhubaneswar, India
[2] School of Physics, Sambalpur University, Jyotivihar, Sambalpur, India
[3] Institute of Physics, Sachivalaya Marg, Bhubaneswar, India

MULTIFRAGMENTATION FISSION IN NEUTRON-RICH URANIUM AND THORIUM NUCLEI

The structural properties of the recently predicted thermally fissile neutron-rich Uranium and Thorium isotopes are studied using the relativistic mean field formalism. The investigation of the new phenomena of multifragmentation fission is analyzed. In addition to the fission properties, the total nuclear reaction cross section which is a measure of the probability of production of these nuclei is evaluated taking ^{6,11}Li and ^{16,24}O as projectiles. The possible use of nuclear fuel in an accelerator based reactor is discussed which may be the substitution of ^{233,235}U and ^{239}Pu for nuclear fuel in near future.

Keywords: relativistic mean field formalism, matter density distribution, nuclear reaction cross section, multi-fragmentation fission.

1. Introduction

The worldwide economic growth shows the requirement of a large amount of energy to fulfill the necessity of the people. In addition to this the existing limited amount of the bio-reservoir, such as coal and petroleum product forces us to think seriously for a sustainable alternative. In this context, the nuclear or solar energy could be the only possible potential substitution for the world's energy requirement. Although the nuclear fusion could be a vast energy source to face any kind of energy deficiency, till date it has not been possible to use it for civilian purpose. It is only so far tested for nuclear weapon as thermonuclear devices (hydrogen bomb). Nevertheless the other nuclear energy source is the nuclear fission which is being used in most of the advanced countries as a viable energy supply.

To get fission energy from heavy elements one has to look for thermally fissile materials in nuclear reactor. There are only three thermally fissile nuclei ^{233,235}U and ^{239}Pu known to the scientific community. Out of these, only ^{235}U is naturally available, whereas ^{233}U and ^{239}Pu are synthesized from ^{232}Th and ^{238}U respectively with a neutron bombarding on it followed by subsequent β-decay from the compound nucleus. In particular, ^{238}U is the major proportion of the fuel material in a thermal reactor, which captures a thermal neutron to produce ^{239}U. ^{239}U quickly emits a β-particle to become ^{239}Np. Then ^{239}Np in turn emits a β-particle to become ^{239}Pu, which is relatively stable and a good candidate for thermally fissile element. Similarly, the synthesis of ^{233}U using ^{232}Th which has a better abundance obtained through the process as

$$n + {}^{232}_{90}Th \rightarrow {}^{233}_{90}Th \xrightarrow{\beta^-} {}^{233}_{91}Pa \xrightarrow{\beta^-} {}^{233}_{92}U.$$

In case of ^{235}U the induced nuclear fission triggers chain reaction producing 2/3 neutrons (average 2.5) with relatively larger fission cross section. One of these neutrons is needed to sustain the chain reaction at a steady level; the other 1.5 is leaked from the core region or absorbed in non-fission reactions. The captured neutron produces energy from this mechanism in the form of gamma rays as the compound nucleus is de-excited. The resultant nucleus becomes more stable by emitting α- or β- particles. It is worthy to emphasize the existence of other thermally fissile Uranium and Thorium neutron-rich isotopes [1, 2]. These newly predicted elements are $^{246\text{-}264}$U and $^{244-262}$Th centering the neutron magic number N = 164 in the superheavy region. These nuclei are capable of producing several orders of magnitude more fission energy than that of ^{233,235}U or ^{239}Pu [1, 2]. This is because of the excess number of neutrons in these neutron-rich thermally fissile isotopes. The excess neutrons are responsible to produce extra neutron fragments at the time of scission and emit few additional prompt neutrons along with the normal fission neutron (similar to the 2.5 neutrons of ^{235}U). The extra neutrons prompt the chain reaction which are vulnerable to thermal neutron fission and produce much more energy compared to ^{233,235}U or ^{239}Pu. The aim of this paper is twofold:

I – To study the structural properties, such as the ground and highly deformed (fission) configuration of predicted thermally fissile nuclei using the relativistic mean field (RMF) formalism.

II – Since the production of these nuclei is crucial, to have an understanding of its synthesis, we have estimated the total nuclear reaction cross section which is a measure of the production probability. In order to synthesize such highly neutron-rich nuclei ($^{242\text{-}262}$Th and $^{244\text{-}264}$U) we need both projectile and target near neutron drip lines. The projectile need to be lower atomic number to overcome the Coulomb barrier. For this reason nuclei like Li and O could be the ideal projectiles. Here we have taken ^{11}Li and ^{24}O as representative cases. The total nuclear reaction cross sections are evaluated by using the RMF densities in the frame-work of Glauber model [3, 4].

The paper is organized as follows. Section 2 gives a brief description of the relativistic mean field formalism and the calculation of total reaction cross section σ_r in the frame-work of Glauber model. In Section 3, we present the detail of our calculated results for the recently predicted thermally fissile nuclei. In this section we have evaluated the nuclear total reaction cross section taking ^{6,11}Li and ^{16,24}O as projectile for the considered U and Th targets. We have also performed dissection of the densities of the neutron-rich U and Th nuclei at different deformation and counted the number of protons and neutrons emitted at the time of thermal fission. The summary and concluding remarks are outlined in Section 4.

2. The Theoretical Framework

The relativistic mean field theory (RMF) in conjunction with Glauber model provides a consistent and confident technique for total nuclear reaction cross-section [5, 6]. Also RMF model shows a good structural agreement with experimental data throughout the periodic table starting from β-stable to drip-line nuclei [7, 8]. The use of RMF formalism for finite nuclei as well as the infinite nuclear matter are well documented and details can be found in [9 - 18]. Here the standard microscopic relativistic Lagrangian is used, where the field for the σ-meson is denoted by σ that for the ω-meson by Vμ and for the isovector ρ-meson by $\mathbf{R}_\mu$ and $\mathbf{A}^\mu$ is the electromagnetic field. The Ψi are the Dirac spinors for the nucleons whose third component of isospin is denoted by τ_{3i}. Here, g_s, g_ω, g_ρ and $e^2/4\pi = 1/137$ are the coupling constants for σ, ω, ρ mesons and photon, respectively. g_2, g_3 and c_3 are the parameters for the nonlinear terms of σ- and ω-mesons. M is the mass of the nucleon and m_σ, m_ω and m_ρ are the masses of the σ, ω and ρ-mesons, respectively. $\mathbf{\Omega}^{\mu\nu}$, $\mathbf{B}^{\mu\nu}$ and $\mathbf{F}^{\mu\nu}$ are the field tensors for the $\mathbf{V}^\mu$, $\mathbf{R}^\mu$ and the photon fields, respectively [9 - 12].

$$L = \overline{\psi}_i\{i\psi^\mu\partial_\mu - M\}\psi_i + \frac{1}{2}\partial^\mu\sigma\partial_\mu\sigma - \frac{1}{2}m_\sigma^2\sigma^2 -$$

$$-\frac{1}{3}g_2\sigma^3 - \frac{1}{4}g_3\sigma^4 - g_s\overline{\psi}_i\psi_i\sigma - \frac{1}{4}\Omega^{\mu\nu}\Omega_{\mu\nu} +$$

$$+\frac{1}{2}m_\omega^2V^\mu V_\mu + \frac{1}{4}c_3(V^\mu V_\mu)^2 - g_\omega\overline{\psi}_i\gamma\psi_iV_\mu - \frac{1}{4}\vec{B}^{\mu\nu}\cdot\vec{B}_{\mu\nu}$$

$$+\frac{1}{2}m_\rho^2\vec{R}^\mu.\vec{R}_\mu - g_\rho\overline{\psi}_i\gamma^\mu\vec{\tau}\psi_i\cdot\vec{R}^\mu -$$

$$-\frac{1}{4}F^{\mu\nu}F_{\mu\nu} - e\overline{\psi}_i\gamma^\mu\frac{(1-\tau_{3i})}{2}\psi_iA_\mu. \qquad (1)$$

From the above Lagrangian, we get the field equations and expression of densities for finite nuclei [9 - 12]. The numerical equations are solved in a self-consistent method using the most successful NL3 parameter set [9 - 13]. The obtained densities are used in the Glauber model for the calculations of total nuclear reaction cross section. The total nuclear reaction cross section at high energies in Glauber model is expressed as [3, 4, 19]:

$$\sigma_r = 2\pi\int_0^\infty b[1-T(b)]db\,, \qquad (2)$$

where T(b) is the transparency function with impact parameter b. The function T(b) is calculated in the overlap region between the projectile and the target with a single NN collision and is given by

$$T(b) = \exp\left[-\sum_{i,j}\overline{\sigma}_{ij}\int d\vec{s}\,\rho_{ij}(s)\,\overline{\rho}_{pj}\left(\left|\vec{b}-\vec{s}\right|s\right)\right], \quad (3)$$

The summation indices i and j run over proton and neutron and subscripts p and t referred to projectile and target, respectively. The experimental nucleon-nucleon reaction cross section σ_{ij} varies with energy. The z-integrated densities $\overline{\rho}(\omega)$ are defined as

$$\overline{\rho}(\omega) = \int_{-\infty}^{\infty}\rho\left(\sqrt{\omega^2+z^2}\right)dz, \qquad (4)$$

with $\omega^2 = x^2 + y^2$. The argument of T(b) in Eq. (2) is $\left|\vec{b} - \overline{s}\right|$ which stands for the impact parameter between the i^{th} and j^{th} nucleons. The original Glauber model was designed for high energy approximation. To take care for low energy case, the Glauber model is modified to the finite range effects in the profile function and Coulomb modified trajectories [4, 20]. The modified T (b) is given by [4, 20 - 23],

$$T(b) = \exp\left[-\int_P \int_T \sum_{ij} \left[\Gamma_{ij}\left(\vec{b} - \vec{s} + \vec{t}\right)\right]\overline{\rho}_{Pi}(\vec{t})\,\overline{\rho}_{Tj}(\vec{s})\,d\vec{s}\,d\vec{t}\right]. \quad (5)$$

Here the profile function Γ_{ij} is given by

$$\Gamma_{ij}\left(b_{eff}\right) = \frac{1 - i\alpha}{2\pi\beta_{NN}^2}\sigma_{ij}\exp\left(-\frac{b_{eff}^2}{2\beta_{NN}^2}\right), \quad (6)$$

where $b_{eff} = \left|\vec{b} - \vec{s} + \vec{t}\right|$, $\vec{b}$ is the impact parameter, $\vec{s}$ and $\vec{t}$ are the dummy variables for integration over the z-integrated target and projectile densities. The values of the parameters, σ_{ij}, α and β_{NN} are usually case-dependent (proton-proton, neutron-neutron or proton-neutron), but we have used the appropriate average values from Refs. [19, 24 - 27].

The deformed or spherical nuclear densities obtained from the RMF model are fitted to a sum of two Gaussian functions with c_i and ranges a_i as coefficients chosen for the respective nuclei which is expressed as

$$\rho(r) = \sum_{i=1}^{N} c_i \exp[-a_i r^2]. \quad (7)$$

Now, the Glauber model is used to calculate the total reaction cross section for the thermally fissile nuclei $^{244\text{-}262}$Th and $^{246\text{-}264}$U as targets.

3. Calculations and Results

First of all we calculate the bulk properties, such as binding energy (B.E), root mean square charge radius r_{ch}, matter radius r_m and quadrupole deformation parameter β_2 for the thermally fissile nuclei $^{242\text{-}262}$Th and $^{244\text{-}264}$U in the RMF formalism. The calculated results are compared with the widely acceptable finite range droplet model (FRDM) [28 - 29] and with the experimental data wherever available [30 - 33] in Table 1. In one of our earlier paper [2] it is shown that the calculated RMF results agree well with the experimental data. Here the investigation is done for highly neutron-rich nuclei where the data are yet to be known. It is clear that our RMF results agree remarkably well with the FRDM values. For example, the RMF binding energy for ^{252}Th and ^{262}U are 1854.2 and 1899.2 MeV as compared to 1853.6 and 1899.0 MeV of the FRDM. Similarly, the β2 values for these two nuclei are 0.199 and 0.118 from RMF with 0.219 and 0.107 from FRDM calculations. In case of ^{264}U the ground state binding energy is 1906.7 MeV in RMF calculation and 1906.0 MeV in FRDM and the corresponding β_2 are −0.089 and −0.138. This means, the ground state is in oblate configuration and inhibit fission. Therefore, we have given the result for first excited prolate configuration in Table 1 which may open for the path of thermal fission.

Table 1. **Calculated results for the binding energy (B. E.), charge and matter radius (r_{ch}, r_m) and deformation parameter (β_2) for various Thorium and Uranium isotopes. The values of finite range droplet model (FRDM) [28 - 29] and experimental data [31 - 33] are also given for comparison. Energy is in MeV and radius is in fm**

Nucleus	B. E.		RMF		β_2	
	RMF	FRDM	r_{ch}	r_m	RMF	FRDM
^{242}Th	1813.3	1816.3	5.912	6.065	0.284	0.235
^{244}Th	1821.0	1824.1	5.921	6.082	0.269	0.225
^{246}Th	1828.6	1831.6	5.926	6.098	0.255	0.217
^{248}Th	1836.1	1839.1	5.926	6.111	0.235	0.209
^{250}Th	1843.5	1846.5	5.929	6.125	0.215	0.209
^{252}Th	1854.2	1853.6	5.938	6.156	0.199	0.219
^{254}Th	1861.9	1859.8	5.946	6.170	0.172	0.192
^{256}Th	1865.4	1864.7	5.955	6.175	0.155	0.088
^{258}Th	1876.0	1871.1	5.965	6.209	0.145	0.088
^{260}Th	1883.0	1877.2	5.973	6.228	0.131	0.098
^{262}Th	1890.1	1883.7	5.981	6.247	0.120	-0.129
^{244}U	1830.4	1832.3	5.937	6.074	0.290	0.235
^{246}U	1838.7	1840.9	5.948	6.093	0.282	0.225
^{248}U	1846.7	1849.1	5.956	6.111	0.271	0.217
^{250}U	1854.5	1857.3	5.960	6.126	0.257	0.218
^{252}U	1864.6	1865.4	5.958	6.147	0.227	0.218

Continuation of Table 1

Nucleus	B. E.		RMF		β_2	
	RMF	FRDM	r_{ch}	r_m	RMF	FRDM
^{254}U	1872.9	1873.1	5.965	6.163	0.207	0.219
^{256}U	1880.9	1880.0	5.973	6.177	0.179	0.201
^{258}U	1888.4	1886.3	5.982	6.196	0.164	0.162
^{260}U	1895.7	1892.7	5.990	6.213	0.147	0.116
^{262}U	1899.2	1899.0	5.996	6.214	0.118	0.107
^{264}U	1903.2	1906.0	5.996	6.230	0.124	-0.138
	1906.7		6.003	6.230	-0.089	

Nucleus	B. E		r_{ch}		r_m	β_2	
	RMF	Exp.	RMF	Exp.	RMF	RMF	FRDM
^{6}Li	44.5	31.99	2.987	2.589 ± 0.039	2.862	0.232	
^{11}Li	54.5	45.71	2.366	2.482 ± 0.043	2.708	0.012	
^{16}O	129.3	127.62	2.877	2.72 ± 0.02	2.741	0.026	0.021
^{24}O	171.6	168.95	2.747		3.054	0.008	0.003

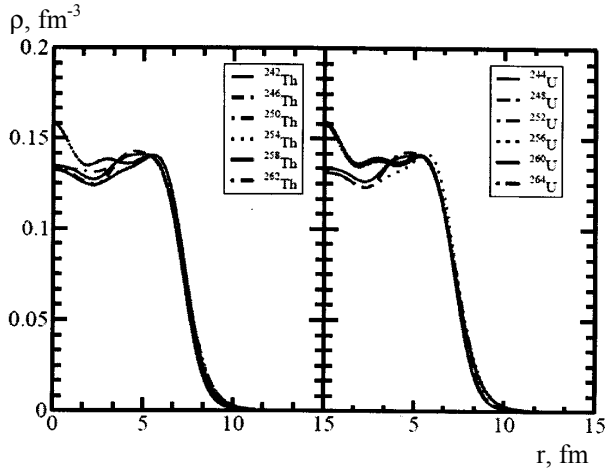

Fig. 1. The total nuclear density obtained by NL3 parameter set [13] for some of the Th and U isotopes.

The spherical densities ρ for Thorium and Uranium isotopes are given in the left and right panel of Fig. 1 respectively. The central part of the density distributions is slightly different from one isotope to other. On the other hand the tail regions are almost identical. The deformed densities obtained from the axially symmetric RMF calculations are converted to spherical equivalent with the help of Eq. (7) and used to calculate the total nuclear reaction cross section σ_r taking ^{6,11}Li and ^{16,24}O as the projectiles. The Gaussian's coefficients c_1, a_1, c_2, a_2 are obtained by converting the deformed density to spherical one using Eq. (7) and are listed in Table 2.

Table 2. **The values of the Gaussian's coefficients obtained by using Eq. (7) from the RMF densities**

Target	RMF(NL3)			
	c_1	a_1	c_2	a_2
^{242}Th	-2.56295	0.046101	2.66072	0.0426229
^{244}Th	-2.57455	0.0458467	2.67157	0.0423937
^{246}Th	-2.58511	0.045586	2.68138	0.0421952
^{248}Th	-2.58381	0.0453282	2.67959	0.0419151
^{250}Th	-2.59781	0.0450663	2.69291	0.0416847
^{252}Th	-2.60123	0.0448158	2.69571	0.0414519
^{254}Th	-2.60059	0.0445618	2.69484	0.0412614
^{256}Th	-2.61142	0.0443161	2.7052	0.0409989
^{258}Th	-2.61164	0.0440842	2.70529	0.040783
^{260}Th	-2.60932	0.0438473	2.70302	0.040563
^{262}Th	-2.61241	0.0435959	2.70652	0.0403415
^{244}U	-2.54329	0.0455993	2.6396	0.0421534
^{246}U	-2.5595	0.0453629	2.655	0.0419438
^{248}U	-2.56618	0.0451347	2.66086	0.04173
^{250}U	-2.59612	0.0448921	2.6908	0.0415151
^{252}U	-2.58623	0.04466	2.67954	0.0412992
^{254}U	-2.59252	0.0444323	2.68509	0.0410873
^{256}U	-2.60491	0.0442003	2.6971	0.0408828
^{258}U	-2.6099	0.0439919	2.70157	0.0406878
^{260}U	-2.63638	0.0437825	2.72829	0.0404995

Continuation of Table 2

Target	RMF(NL3)			
	c_1	a_1	c_2	a_2
^{262}U	-2.64603	0.0435736	2.73785	0.0403142
^{264}U	-2.64126	0.0433618	2.73345	0.0401156
^{6}Li	-1.2017	0.0338401	0.467028	0.0338391
^{11}Li	-0.054061	0.0628475	0.231925	0.0231428
^{16}O	-2.24049	0.035433	2.37892	0.0314394
^{24}O	-1.92109	0.0267916	2.07684	0.0235596

In order to synthesize such highly neutron rich nuclei ($^{242\text{-}262}$Th and $^{244\text{-}264}$U), we need neutron rich projectile as well as target. For this reason, we have taken ^{11}Li and ^{24}O as projectiles during the calculation of the total nuclear reaction cross section for the compound nucleus. These combinations of projectile and target in the nuclear reaction, are taken here as a representative case. It is well known that the neutron rich nuclei are not stabilized by nature but it is possible to synthesize in laboratory. Also we look for σ_r for stable projectile of same atomic number with the respective targets and the results are displayed in Figs. 2 and 3.

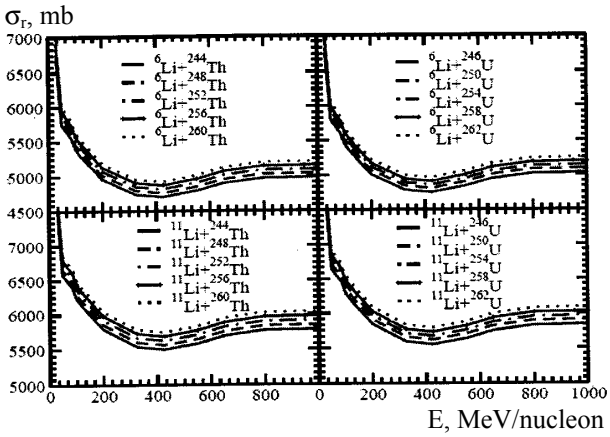

Fig. 2. The total nuclear reaction cross-section σ_r (mb) for thermally fissile $^{244\text{-}260}$Th and $^{246\text{-}262}$U target with ^{6,11}Li as projectiles at different incident energies.

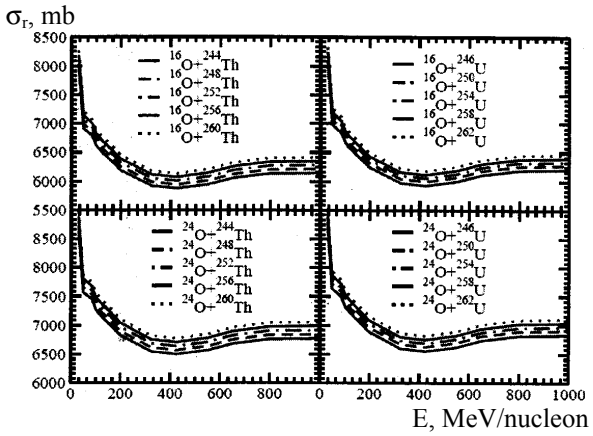

Fig. 3. The same as Fig. 2 but with ^{16,24}O projectile.

The variation σ_r per two neutrons in the Th-isotopic chain are ~ 28 - 30 mb for ^{6}Li, ~ 31 - 33 mb for ^{11}Li, ~ 32 - 36 mb for ^{16}O and ~ 35 - 37 mb for ^{24}O. Similarly for Uranium target, these changes are ~ 22 - 33 mb for ^{6}Li, ~ 25 - 34 mb for ^{11}Li, ~ 27 - 34 mb for ^{16}O and ~ 29 - 36 mb for ^{24}O. Interestingly, increase of σ_r is least from ^{250}U to ^{252}U for these four projectiles. A further inspection of σ_r shows, the rate of increase is large for ^{6}Li to ^{11}Li than ^{16}O to ^{24}O. These results are depicted in Table 3. It is clear from the figures, the σ_r decreases with incident energy and again increases slightly. At about 600 MeV, it becomes stable up to 1000 MeV or more. Similar to our earlier investigation [5, 6], σ_r increases with target mass in the isotopic chain for both Th and U isotopes. In other word, the σ_r directly proportional to the formation probability of the nuclei.

The increase in reaction cross-section with mass number could be a finite possibility to synthesize such neutron rich nuclei and which may play an important role for power generation in near future. Right now the formation of such a neutron-rich heavy nuclei looks like hypothetical. However after the completion of Facility for Antiproton and Ion Research (FAIR) [34] at GSI, Germany, there is every possibility for an accelerator based reactor where these thermally fissile neutron-rich Thorium and Uranium nuclei could be a viable nuclear fuel for the power generation of the entire world.

Table 3. **The total nuclear reaction cross-section σ_r (mb) for thermally fissile $^{244-262}$Th and $^{246-264}$U target with ^{6,11}Li and ^{16,24}O projectiles at energy 800 MeV**

Target	σ_r, mb for Projectile			
	^{6}Li	^{11}Li	^{16}O	^{24}O
^{242}Th	4942.09	5737.91	6099.93	6723.97
^{244}Th	4970.99	5769.79	6133.19	6759.56
^{246}Th	5000.51	5802.37	6167.53	6795.97

Continuation of Table 3

Target	σ_r, mb for Projectile			
	^{6}Li	^{11}Li	^{16}O	^{24}O
^{248}Th	5030.03	5835.32	6201.96	6832.49
^{250}Th	5059.62	5867.68	6236.42	6869.02
^{252}Th	5089.12	5900.26	6270.77	6905.42
^{254}Th	5118.17	5932.38	6304.70	6941.40
^{256}Th	5146.73	5963.91	6337.95	6976.64
^{258}Th	5174.45	5994.52	6370.29	7010.85
^{260}Th	5202.25	6025.25	6402.09	7045.25
^{262}Th	5230.00	6056.00	6435.22	7079.75
^{244}U	4990.78	5792.15	6157.39	6785.40
^{246}U	5018.75	5823.02	6189.85	6819.84
^{248}U	5046.81	5853.94	6222.37	6854.29
^{250}U	5081.38	5891.66	6261.66	6895.75
^{252}U	5103.77	5916.74	6288.48	6924.32
^{254}U	5132.12	5947.98	6321.36	6959.13
^{256}U	5159.70	5978.38	6353.39	6993.05
^{258}U	5186.43	6007.81	6384.34	7025.81
^{260}U	5218.94	6043.22	6421.15	7064.60
^{262}U	5244.57	6071.46	6450.88	7096.07
^{264}U	5270.15	6099.72	6480.70	7127.66

The half life-time (T_{β}^{-}) of the considered nuclei is expected to be small because of β-decay. For example, T_{β}^{-} for ^{248}U and ^{250}U are 5.62 and 3.28 s and for ^{246}Th and ^{248}Th are 1.44 and 0.66 s respectively. But the production of these nuclei via accelerator and their direct use in the reactor for power generation will be an ideal technical design. A comparison of our results with FRDM [28] results for β decay energy Q_{β} and half life-time T_{β}^{-} of $^{242-262}$Th and $^{244-264}$U are tabulated in Table 4.

Table 4. **Comparison of RMF and FRDM [28] results for β decay energy Q_{β} and half life-time T_{β}^{-} of $^{242-262}$Th and $^{244-264}$U**

Nucleus	Q_{β}		T_{β}^{-}		Nucleus	Q_{β}		T_{β}^{-}	
	RMF	FRDM	RMF	FRDM		RMF	FRDM	RMF	FRDM
^{242}Th	5.519	2.71	7.124	14.507	^{244}U	4.446	1.49	33.513	>100
^{244}Th	6.025	3.86	1.829	2.855	^{246}U	5.017	2.70	10.800	20.068
^{246}Th	6.46	4.09	1.443	2.279	^{248}U	5.508	3.14	5.623	9.863
^{248}Th	6.851	4.66	0.657	0.967	^{250}U	5.923	3.44	3.277	5.642
^{250}Th	7.172	4.98	0.452	0.65	^{252}U	6.395	3.81	1.748	2.934
^{252}Th	7.431	5.50	0.279	0.377	^{254}U	6.717	4.38	0.836	1.282
^{254}Th	7.544	6.32	0.167	0.20	^{256}U	6.944	5.24	0.499	0.661
^{256}Th	7.821	7.43	0.026	0.271	^{258}U	6.892	5.83	0.230	0.272
^{258}Th	8.309	6.68	0.056	0.07	^{260}U	6.656	6.04	0.120	0.133
^{260}Th	8.961	7.14	0.049	0.062	^{262}U	7.06	6.33	0.108	0.120
^{262}Th	9.501	6.73	0.087	0.123	^{264}U	6.594	5.83	0.233	0.264

It is well-known that 2.5 average numbers of neutrons emit from the ^{235}U in the thermal fission process. This number is more than twice for ^{250}U [1, 2], which integrate the thermal fission process and produce more energy of the order of magnitude. It is worth mentioning that in multifragmentation fission along with the usual two big fragments [which we are used to] a few (about 3 neutrons in case of ^{250}U) neutrons come out from the fission process [1, 2]. In case of ^{250}U on an average 5.5 neutrons will evolve. That is 3 multifragmentation neutrons and 2.5 prompt neutrons will come out per fission process. To be more specific, in case of ^{235}U, we get only 2.5 prompt neutrons and no multifragmentation neutrons.

In these highly neutron rich compound nucleus, the fragments after fission have the same atomic number but highly neutron rich than that the fragments evolves from $^{233\text{-}235}$U and ^{239}Pu. As a result the nuclei (fragments) formed after fission crosses the boundary of nuclear chart (the drip line) and unable to accept these excess neutrons and evolves as multifragmentation fission neutrons.

Now it is obvious that 5.5 prompt neutrons

participate in the chain reaction in case of ^{250}U compared to the 2.5 neutrons of ^{235}U. As a result, neutron-rich thermally fissile nuclei reach to the critical stage much faster than the normal thermally fissile material like ^{233,235}U and ^{239}Pu. This phenomenon can be illustrated by counting the number of neutron emerging from the multifragmentation fission. For this, we have shown the contour plot of density distribution for selective cases ^{244,254,262}Th and ^{244,254,264}U in Figs. 4 and 5.

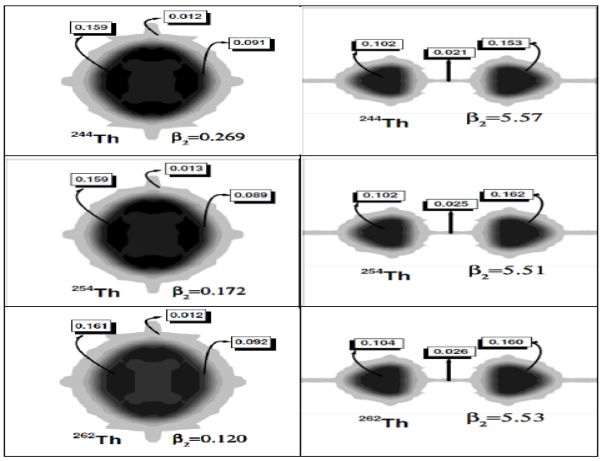

Fig. 4. The evolution of neck configuration for ^{244,254,262}Th, i.e., the total density ρ at ground state and in the scission configuration.

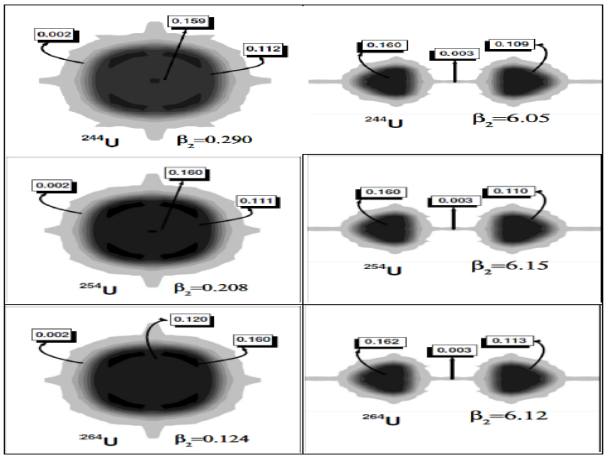

Fig. 5. The evolution of neck configuration for ^{244,254,264}U, i.e., the total density ρ at ground state and in the scission configuration.

Table 5. **Anatomy of neck at the fission configuration for ^{244,254,262}Th and ^{244,254,264}U**

Nucleus	Range of Neck		Neck Nucleons		N_n/N_p	r_{ch}^{neck}	l_{neck}
	z	ρ	N_p	N_n			
^{244}Th	±1.039	±2.45	0.7	2.67	3.81	11.86	4.72
^{254}Th	±1.044	±2.43	0.7	3.4	4.86	11.77	4.63
^{262}Th	±1.043	±2.41	0.9	3.9	4.33	11.70	4.45
^{244}U	±1.018	±2.38	0.8	2.7	3.38	12.09	6.18
^{254}U	±1.018	±2.38	0.9	3.7	4.11	11.76	5.65
^{264}U	±1.020	±2.36	1.02	5.47	5.02	11.72	4.14

N o t e. Here z and ρ are the range of the neck where we have counted the number of neutron N_n, proton N_p and their ratio. l_{neck} and r_{ch}^{neck} stand for length of the neck and charge radius of the nucleus in fm.

We concentrate on the neck region of the contour curve at the fission (or near fission) state ($\beta_2 \sim 6.0$). By integrating the density of that portion, we get the number of nucleons present in the neck. Also, we have calculated the length of the neck l_{neck}, the number of neck nucleons (proton N_p and neutron N_n) and their ratio N_n/N_p for ^{244,254,262}Th and ^{244,254,264}U, which are given in Table 5. The neck length l_{neck} (or area) almost remains same (or decreases slightly) with mass number of a nucleus, but the availability of nucleons and their ratio increases. For example, N_n = 2.673 and 2.7 for ^{244}Th and ^{244}U and these numbers are 3.9 and 5.5 for ^{262}Th and ^{264}U. This says about the increase of multiplicity of neutron number at the time of fission for neutron-rich nuclei. This will be responsible for the increase of chain reaction at the time of power production with such fuels. To have a better understanding about the neck evolution, the analysis can be done from the density distribution at various quadrupole deformation parameter β_2 (see Figs. 4 and 5). At large deformation the nucleus divided into two major fragments along with the emission of few more neutrons from the neck. Because of the large number of neutron emission (multifragmentation fission) at the time of fission, the critical mass of these nuclear fuel is expected to be small, which may be an extra mileage for collection of such materials.

4. Summary and Conclusion

In summary, we have studied the structural properties of the recently predicted thermally fissile neutron-rich $^{242-262}$Th and $^{244-264}$U nuclei in the frame-work of RMF model and possible solution of energy crisis. The results are compared with the most popular FRDM calculations and found remarkably closure with the predictions. The obtained RMF densities are used to estimate the total nuclear reaction cross section which is a measure of the production probability, taking these fissile

isotopes as target with ^{6,11}Li and ^{16,24}O as projectile.

These results may be useful for experimentalists for the synthesis of neutron rich thermally fissile Thorium and Uranium for the energy generation in future. The anatomy of the fission process is done with the help of the neck configurations. The maximum number of multifragmentation neutron at the time of fission is found to be more with larger neutron-rich nuclei. This will certainly increase the efficiency of the chain reaction during the fission process and will reduce the critical mass of the nuclear fuel, if neutron-rich thermally fissile nuclei will be used as nuclear fuel in an accelerator based nuclear reactor.

REFERENCES

1. *Satpathy L., Patra S.K., Choudhury R.K.* Fission decay properties of ultra neutron-rich uranium isotope // PRAMANA - J. Phys. - 2008. - Vol. 70. - P. 87 - 99.
2. *Patra S.K., Choudhury R.K., Satpathy L.* Anatomy of neck configuration in fission decay // J. Phys. - 2010. - Vol. G37. - P. 085103 - 085117.
3. *Glauber R.J.* Lectures on Theoretical Physics / Ed. by Brittin W. E and Dunham L. C. - New York: Interscience, 1959. - Vol. 1. - 315 p.
4. *Abu-Ibrahim B., Ogawa Y., Suzuki Y., Tanihata I.* Cross section calculations in Glauber model: I. core plus one nucleon case // Comp. Phys. Comm. - 2003. - Vol. 151. - P. 369 - 386.
5. *Patra S.K., Panda R.N., Arumugam P., Gupta Raj K.* Nuclear reaction cross sections of exotic nuclei in the Glauber model for relativistic mean field densities // Phys. Rev. - 2009. - Vol. C80. - P. 064602 - 064613.
6. *Panda R.N., Patra S.K.* Formation of neutron-rich and superheavy elements in astrophysical objects // J. Mod. Phys. - 2010. - Vol. 1. - P. 312 - 318.
7. *Patra S.K., Praharaj C.R.* Relativistic mean field study of light medium nuclei away from beta stability // Phys. Rev. - 1991. - Vol. C44. - P. 2552 - 2565.
8. *Gambhir Y.K., Ring P., Thimet A.* Relativstic mean field theory for finite nuclei // Ann. Phys. (N.Y.) - 1990. - Vol. 198. - P. 132 - 179.
9. *Boguta J., Bodmer A.R.* Relativistic calculation of nuclear matter and nuclear surface // Nucl. Phys. - 1977. - Vol. A292. - P. 413 - 428.
10. *Miller L.D., Green A.E.S.* Relativistic self-consistent meson field theory of spherical nuclei // Phys. Rev. - 1972. - Vol. C5. - P. 241- 252.
11. *Walecka J.D.* A theory of highly condensed matter // Ann. of Phys. - 1974. - Vol. 83. - P. 491 - 529.
12. *Pannert W., Ring P., Boguta J.* Relativistic mean-field theory and nuclear deformation // Phys. Rev. Lett. - 1987. - Vol. 59. - P. 2420 - 2422.
13. *Lalazissis A.G., König J., Ring P.* New parametrization for the Lagrangian density of relativistic mean field theory // Phys. Rev. - 1997. - Vol. C55. - P. 540 - 543.
14. *Estal Del M., Centelles M., Vĩnas X., Patra S.K.* Pairing properties in relativistic mean field models obtained from effective field theory // Phys. Rev. - 2001. - Vol. C63. - P. 044321 - 044334.
15. *Patra S.K., Estal Del M., Centelles M., Vĩnas X.* Ground-state properties and spins of the odd $Z = N + 1$ nuclei ^{61}Ga-^{97}In // Phys. Rev. - 2001. - Vol. C63. - P. 024311 - 024317.
16. *Estal Del. M., Centelles M., Vi˜nas X. and Patra S. K.* Effects of new nonlinear couplings in relativistic effective field theory // Phys. Rev. - 2001. - Vol. C63. - P. 024314 - 024324.
17. *Arumugam P., Sharma B.K., Sahu P.K. et al.* // Phys. Lett. - 2004. - Vol. B601. - P. 51 - 55.
18. *Serot B.D., Walecka J.D.* Recent progress in quantum hadrodynamics // Int. J. Mod. Phys. - 1997. - Vol. E6. - P. 515 - 631.
19. *Karol P.J.* Nucleus-nucleus reaction cross sections at high energies: Soft-spheres model // Phys. Rev. - 1975. - Vol. C11. - P. 1203 - 1209.
20. *Shukla P.* Glauber model and the heavy ion reaction cross section // Phys. Rev. - 2003. - Vol. C67. - P. 054607 - 054613.
21. *Bhagwat A., Gambhir Y.K.* Microscopic description of recently measured reaction cross sections of neutron-rich nuclei in the vicinity of the $N = 20$ and $N = 28$ closed shells // Phys. Rev. - 2008. - Vol. C77. - P. 027602 - 027605.
22. *Bhagwat A., Gambhir Y.K.* Recently measured reaction cross sections with low energy fp-shell nuclei as projectiles: Microscopic description // Phys. Rev. - 2006. - Vol. C73. - P. 054601 - 054606.
23. *Bhagwat A., Gambhir Y.K.* Microscopic investigations of mass and charge changing cross sections // Phys. Rev. - 2004. - Vol. C69. - P. 014315 - 014325.
24. *Charagi S.K., Gupta S.K.* Coulomb-modified Glauber model description of heavy-ion reaction cross sections // Phys. Rev. - 1990. - Vol. C41. - P. 1610 - 1618.
25. *Charagi S.K., Gupta S.K.* Coulomb-modified Glauber model description of heavy-ion elastic scattering at low energies // Phys. Rev. - 1992. - Vol. C46. - P. 1982 - 1987.
26. *Charagi S.K.* Nucleus-nucleus reaction cross section at low energies: Modified Glauber model // Phys. Rev. - 1993. - Vol. C48. - P. 452 - 454.
27. *Charagi S.K., Gupta S.K.* Nucleus-nucleus elastic scattering at intermediate energies: Glauber model approach // Phys. Rev. - 1997. - Vol. C56. - P. 1171 - 1174.
28. *Möller P., Nix J.R., Kratz K.-L.* Nuclear properties for astrophysical and radioactive ion- beam applications // At. Data Nucl. Data Tables. - 1997. - Vol. 66. - P. 131 - 343.
29. *Möller P., Nix J.R.* Nuclear ground state masses and deformations // At. Data Nucl. Data Tables. - 1995. - Vol. 59. - P. 185 - 381.
30. *Audi G., Wapstra A.H., Thebault C.* The AME2003 atomic mass evaluation // Nucl. Phys. - 2003. - Vol. A729. - P. 337 - 676.
31. *Nortershauser W., Neff T., Sanchez R., Sick I.* Charge radii and ground state structure of lithium isotopes:

Experiment and theory reexamined // Phys. Rev. - 2011. - Vol. C84. - P. 024307 - 024320.
32. *Dubler T. et al.* Nuclear charge radii from X-ray transitions in muonic atoms of carbon, nitrogen and oxygen // Nucl. Phys. - 1974. - Vol. A219. - P. 29 - 38.
33. *Audi G., Wang Meng* // Private communication. - April 2011.
34. *Friese V., Sturm C.* CBM Progress report ISBN 978-3-9811298-8-5. - 2010. (www.gsi.de); www.fair-center.eu.

Р. Н. Панда, М. Буян, С. К. Патра

БАГАТОЧАСТИНКОВИЙ ПОДІЛ НЕЙТРОННО-НАДЛИШКОВИХ ЯДЕР УРАНУ ТА ТОРІЮ

У рамках релятивістської теорії середнього поля вивчаються структурні властивості недавно передбачених нейтронно-надлишкових ізотопів урану та торію. Аналізуються дослідження нового явища – багаточастинкового поділу. Поряд із властивостями поділу розраховано повні перерізи ядерних реакцій, що є мірою ймовірності утворення цих ядер, з налітаючими іонами ^{6,11}Li та ^{16,24}O. Обговорюється можливість використання нейтронно-надлишкових ізотопів урану та торію в реакторах майбутнього замість ^{233,235}U та ^{239}Pu.

Ключові слова: релятивістська теорія середнього поля, розподіл густини речовини, переріз ядерної реакції, багаточастинковий поділ.

Р. Н. Панда, М. Буян, С. К. Патра

МНОГОЧАСТИЧНОЕ ДЕЛЕНИЕ НЕЙТРОННО-ИЗБЫТОЧНЫХ ЯДЕР УРАНА И ТОРИЯ

В рамках релятивистской теории среднего поля изучаются структурные свойства недавно предвиденных нейтронно-избыточных изотопов урана и тория. Анализируются исследования нового явления – многочастичного деления. Наряду со свойствами деления рассчитаны полные сечения ядерных реакций, что является мерой вероятности образования этих ядер, с налетающими ионами ^{6,11}Li и ^{16,24}O. Обсуждается возможность использования нейтронно-избыточных изотопов урана и тория в реакторах будущего вместо ^{233,235}U и ^{239}Pu.

Ключевые слова: релятивистская теория среднего поля, распределение плотности вещества, сечение ядерной реакции, многочастичное деление.

Надійшла 10.05.2012
Received 10.05.2012